Thermal characterisation of an ammonia-charged two-phase closed thermosyphon

R.T. Dobson[1] and **D.G. Kröger**

(*First received October 1999; Final version April 2000*)

The thermal performance characteristics including the evaporator and condenser heat transfer coefficients and the maximum heat transfer rate for an ammonia charged two-phase closed thermosyphon have been experimentally determined for vertical and inclined orientations. The thermosyphon tested is 6.2 m long and has an internal diameter of 31.9 mm and is made of grade 304 stainless steel. Hot water of up to 80° C and cooling water of between 10 and 20° C, inclination angles of 30, 45, 60, 75 and 90° to the horizontal, evaporator to total length ratios of 0.06 to 0.33 and liquid charge fill ratios (L_ℓ/L_e) of between 20 and 100 % were considered. The correlations of the experimental data for the heat transfer coefficients are given in terms of the wall heat flux, internal pressure, liquid charge fill ratio and angle of inclination. The correlation for the superficial velocity at which the heat transfer rate could not be increased further by increasing the temperature difference between the evaporator and the condenser was determined in terms of internal temperature, liquid charge fill ratio and inclination angle. The experimentally determined values of the heat transfer coefficients did not correspond well with existing correlations. This is attributed to the limited availability of ammonia as working fluid and inclined thermosyphon orientations in the data sets upon which these existing correlations were based, as well as the generally complex nature of the various heat transfer mechanisms that occur in a thermosyphon.

Nomenclature

A	area, m^2
d	diameter, m
h	heat transfer coefficient, W/m^2K
h_{fg}	latent heat of vaporisation, J/kg
k	thermal conductivity, W/mK
L	length, m
$\dot{m}$	mass flow rate, kg/s
P	pressure, Pa
$\dot{q}$	heat transfer rate, W
$\dot{q}''$	heat transfer flux, W/m^2
r	correlation coefficient
T	temperature, °C
V	velocity

Subscripts

b	bottom
c	cold, cooling or condenser
e	evaporator or exit
h	hot or heating
i	inside or inlet
ℓ	liquid
o	outside
s	superficial
t	top
v	vapour, velocity
w	wall

Greek symbols

ϕ	inclination angle (to the horizontal)
ρ	density, kg/m^3
μ	viscosity, kg/ms

Introduction

The two-phase closed thermosyphon is a simple yet effective heat transfer device.[1] It consists of a sealed pipe containing both liquid and vapour phases of a relatively small amount of a working fluid. When the lower end of the pipe relative to gravity is heated and the higher end cooled, heat is transferred between the two ends. The heat transfer rate between the two ends is considerably more than would be the case for the same diameter solid rod of conducting material subjected to the same temperature difference.

Evaporation of the liquid takes place in the heated portion of the pipe and this portion is hence also termed the evaporating section or evaporator or boiler. In the cooled portion the vapour condenses and is termed the condensing section or condenser. In the condenser the working fluid changes phase from vapour to liquid and more vapour flows from the evaporator to the condenser. The condensate formed in the higher portion of the pipe then runs down the inside of the wall, under the influence of gravity, to replenish the pool of boiling liquid in the lower portion of the pipe.

As the temperature difference between the heated and cooled ends increases so too does the heat transfer rate and the velocity of the upwardly flowing vapour. A further increase in temperature difference ultimately leads to a maximum possible or limiting heat transfer condition. This limiting condition may be ascribed to one or a combination of effects: *flooding* whereby the upwardly flowing vapour

[1]Department of Mechanical Engineering, University of Stellenbosch, Private Bag X1, Matieland, 7602 South Africa

prevents an adequate flow of the downwardly flowing condensate back into the evaporator; *geysering* whereby liquid is propelled directly out of the evaporator and up into the condensing section by the rapid flow of the vapour; and *dryout* whereby liquid deficient areas occur on the evaporating surface. The occurrence of any of these effects does not necessarily imply that the thermosyphon is operating at this limiting condition. For instance[2] flooding may be observed to be occurring and yet the heat transfer rate may still be increased further by increasing the temperature difference between the evaporator and condenser.

The physical phenomena describing the thermal-hydraulic behaviour taking place within the thermosyphon, especially if it is inclined, are relatively complex. Figure 1 gives an indication of the various processes taking place in an inclined thermosyphon. To date theoretical analysis has been limited to only vertically orientated thermosyphons in which the condensate is assumed to form a uniform axi-symmetrical annular film of varying thickness on the inside wall of the pipe. There are many correlations relating to the thermal performance characteristics of thermosyphons.[3] These correlations, however, give widely differing results.[4]

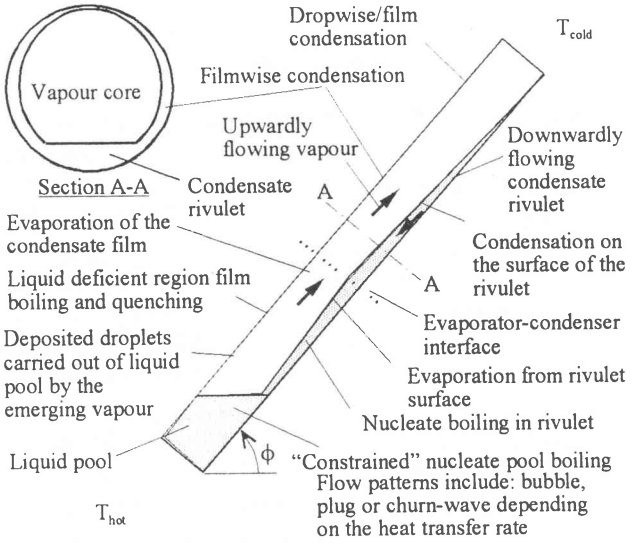

Figure 1 Heat transfer mechanisms in an inclined thermosyphon

Ammonia is an attractive working fluid for use in a closed two-phase thermosyphon because of its zero ozone depletion and its zero global warming potentials. It has good thermal properties and the refrigeration industry has had extensive experience with it. Its thermal and heat transfer characteristics are significantly better than those of CFCs and HCFCs and are comparable to those of water. Although ammonia has been used for decades as a refrigerant of choice for selected large and small scale applications, no formal database is available on the heat transfer of ammonia.[5] Very little published data relating to ammonia's heat transfer characteristics are available and in the case of an inclined ammonia-charged thermosyphon no published data are available.

In this paper the important thermal characteristics of an ammonia charged two-phase closed thermosyphon are experimentally determined for both vertical and inclined orientations. The important thermal characteristics are the evaporator and condenser heat transfer coefficients and the maximum heat transfer rate.

Experimental set-up and procedure

The thermosyphon tested consists of a 6.2 m long by 31.9 mm inside diameter stainless steel pipe. It is mounted in a support structure that can be tilted at 30, 45, 60, 75, and 90° to the horizontal. The thermosyphon has five 400 mm and one 4 200 mm water heating and cooling jackets as shown in Figure 2. By coupling these water jackets in different combinations it is possible to operate the thermosyphon with different evaporator and condenser lengths. During a test run the heating water from the hot water supply tank, as shown in Figure 3, was increased from the initial temperature up to a maximum of about 80°C and the cooling water was allowed to vary from between 10 and 20°C.

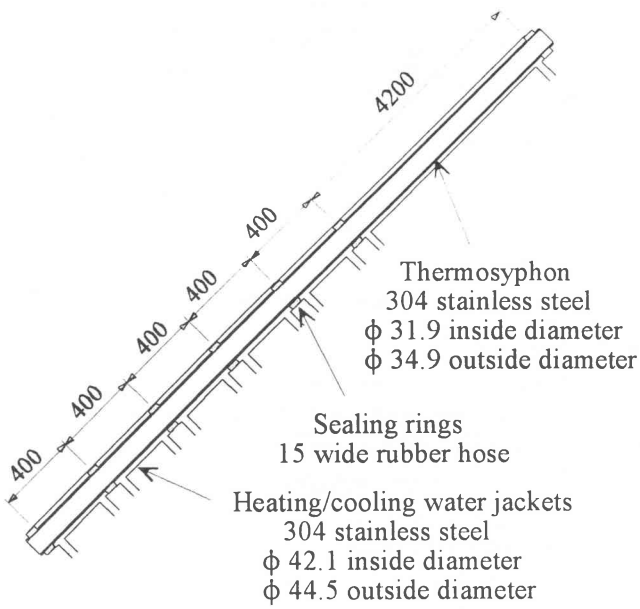

Figure 2 Thermosyphon heating and cooling (dimensions in mm)

Mass flow rates were determined by measuring the time it takes for a measured mass of water to flow. Temperature was measured using T-type stainless steel sheathed thermocouple probes all manufactured from the same batch of themocouple wire. Temperatures were recorded using a Schlumberger Technologies data acquisition system ("IMP PC to S-net Adapter") coupled to

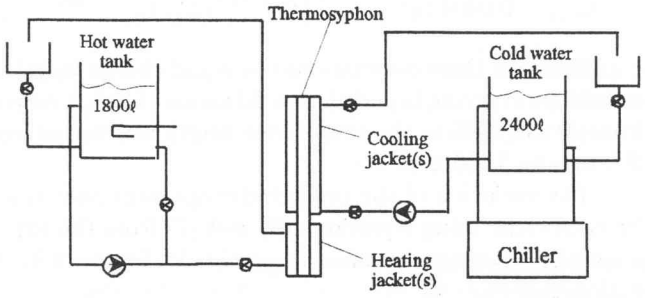

Figure 3 Thermosyphon heating and cooling water systems

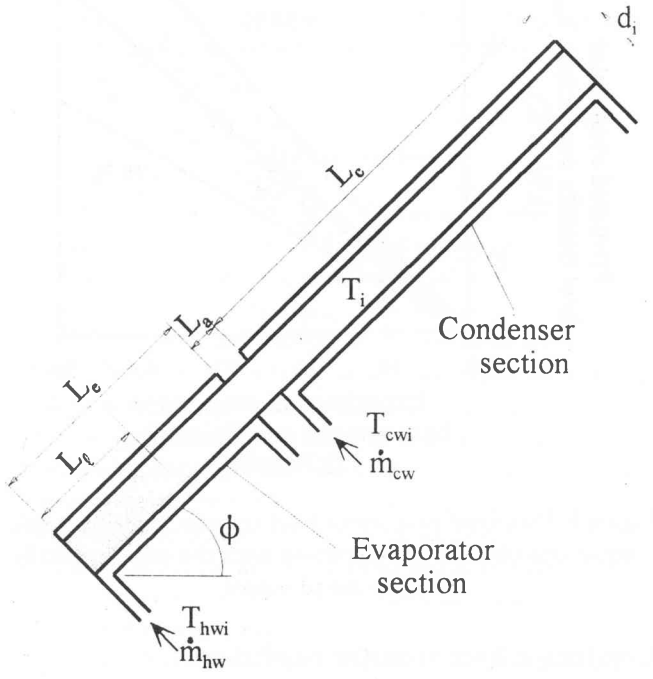

Figure 4 Important independent variables for an inclined thermosyphon

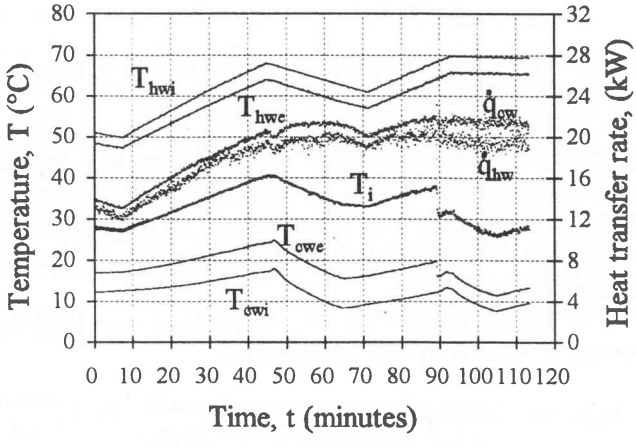

Figure 5 Typical set of readings fora test run

a PC. The independent experimental variables L_e, L_c, L_ℓ, T_{hwi}, T_{cwi}, Φ, $\dot{m}_{hw}$ and $\dot{m}_{cw}$ are shown in Figure 4.

The logged data (heating and cooling water inlet and exit temperatures as well as the ammonia temperature at the bottom and top of the thermosyphon) were recorded every 30 seconds and a plot of a typical set of readings and results is shown in the Figure 5. A test run continued until the maximum heat transfer rate occurred or the maximum achievable temperature of the hot water heating system of 80°C had been reached. The minimum cooling water temperature that the cooling system could supply was about 8°C. For each test run between four and six more or less equally spaced points were selected to make up the data set on which the heat transfer coefficients were calculated. In all there were about 70 such test runs from which a data set of some 280 points was extracted upon which to base the heat transfer coefficient correlations. There were five inclination angles (30, 45, 60, 75, and 90°), three liquid charge lengths (396, 784 and 1 296 mm) and five evaporator leiigths (400, 800, 1 200, 1 600 and 2 000 mm). There was no adiabatic length and the condenser lengths are given by subtracting the evaporator lengths from the overall length of 6.2 m giving condenser lengths of 4.2, 4.6, 5.0, 5.4 and 5.8 m. Depending on the heating and cooling temperatures the internal ammonia temperatures varied from 15 to 45°C.

A total of 48 points were available on which to base the maximum heat transfer rate correlation. Although there were 70 test runs it was not possible, due to the maximum water heating and minimum cooling water limitations of the heating/cooling water equipment, to obtain a clearly observable maximum heat transfer rate for the inclined cases with heating water flowing through only a single 400 mm water jacket.

The average heat flux and inside wall temperature of the heated and cooled sections of the thermosyphon were determined from the measurements. This allowed the evaporator and condenser heat transfer coefficients to be determined by dividing the heat flux by the temperature difference between the inside of the wall and the temperature of the working fluid as follows:

$$h_{wie} = \frac{\dot{q}''_{wie}}{T_{wie} - T_i}, \text{ and} \tag{1}$$

$$h_{wic} = \frac{\dot{q}''_{wic}}{T_i - T_{wic}} \tag{2}$$

where

$$\dot{q}''_{wie} = \frac{\dot{q}_e}{A_{wie}}, \quad \dot{q}''_{wic} = \frac{\dot{q}_c}{A_{wic}}$$

$$\dot{q}_e = \dot{m}_{hw} c_{phw@\overline{T}_{hw}} (T_{hwe} - T_{cwi}),$$
$$\dot{q}_c = \dot{m}_{cw} c_{pcw@\overline{T}_{cw}} (T_{cwi} - T_{cwe}),$$

$$A_{wie} = \pi d_i L_e, \; A_{wic} = \pi d_i L_c$$

$$T_{wie} = \overline{T}_{hw} - \left(\frac{1}{h_{woe}A_{woe}} + \frac{\ln(d_o/d_i)}{2\pi k_{we}L_e}\right)\dot{q}_e,$$
$$T_{wic} = \overline{T}_{cw} + \left(\frac{1}{h_{woc}A_{woc}} + \frac{\ln(d_o/d_i)}{2\pi k_{wc}L_c}\right)\dot{q}_c$$

$$\overline{T}_{hw} = \frac{T_{hwi}+T_{hwe}}{2},\ \overline{T}_{cw} = \frac{T_{cwi}+T_{cwe}}{2},$$
$$A_{weo} = \pi d_o L_e \text{ and } A_{wco} = \pi d_o L_c$$

The heat transfer coefficient between the heating water and the outside surface of the thermosyphon for a 400 mm long water jacket was experimentally determined as[6]

$$h_{ewo} = 4.553 \underset{hw}{\text{Re}}^{0.7333} \text{Pr}_{hw}^{0.3626} \quad (3)$$

and from the outside surface to the cooling water as

$$h_{wco} = 2.029 \underset{cw}{\text{Re}}^{0.8095} \text{Pr}_{cw}^{0.3774} \quad (4)$$

Because of the relatively low thermal conductivity of stainless steel (304) the temperature difference across the wall is relatively large and contributes significantly to the overall resistance to heat transfer. The thermal conductivity of stainless steel is relatively sensitive to temperature changes and hence its thermal conductivity was determined as a function of temperature as

$$k_w = 9 + 0.02\,(T_w + 273.15) \quad (5)$$

where k is in W/mK if T_w is in °C. The wall temperature in equation (5) was taken as the average temperature of heating/cooling water and the internal temperature of the working fluid.

Experimental results

The experimental data were correlated by assuming correlating equations of the form

$$y = a_0\,(x_1)^{b_1}\,(x_2)^{b_2}\,(x_3)^{b_3}\ \ldots\ldots$$

By taking logs on both sides, the coefficients are readily calculated making use of multi-linear regression. In this way correlations were obtained for the evaporator and condenser heat transfer coefficients and the maximum superficial vapour velocity above which the heat transfer rate could not be increased further.

Evaporator heat transfer coefficient

An evaporator heat transfer coefficient for inclination angles of 30 to 75° (based on a data set of 125 points and with $r^2 = 94.4\%$) was determined as[7]

$$h_{ewi} = 0.413\,(\dot{q}''_{ewi})^{0.980}\,(P_i)^{-0.455}\,(L_\ell/L_e)^{0.305}\sin^{0.351}\phi \quad (6)$$

where h is in kW/m^{2}K if $\dot{q}''$ is in kW/m^2, P_i in bar, and L_ℓ/L_e in m/m.

For a vertically orientated geometry based on a data set of 49 points and $r^2 = 98.2\%$ it was determined as

$$h_{ewi} = 0.0404\,(\dot{q}''_{ewi})^{0.931}\,(P_i)^{0.615}\,(L_\ell/L_e)^{-0.290} \quad (7)$$

For both these correlations the liquid charge length L_ℓ was 400 mm giving liquid charge fill ratios (L_ℓ/L_e) varying from 20 to 100 % as the evaporator length was varied from 400 mm to 2 000 mm.

The variation of the predicted evaporator heat transfer coefficient using equations (6) and (7) from the experimentally determined values is shown in Figure 6 to be within ±30 %.

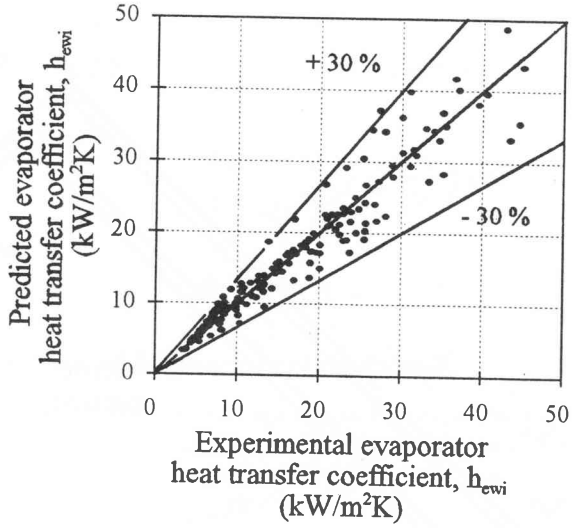

Figure 6 Predicted evaporator heat transfer coefficient using equations (6) and (7) compared with the experimentally determined values

Condenser heat transfer coefficient

For the vertical case the experimental data were correlated (49 data points and $r^2 = 72.6\%$) as

$$h_{cwi} = 0.3706\,(\dot{q}''_{cwi})^{0.0861}\,(P_i)^{-0.2429}\,(L_c)^{1.3523} \times (L_\ell/L_e)^{-0.3474} \quad (8)$$

where h is in kW/m^{2}K if $\dot{q}''$ is in kW/m^2, P_i in bar, L_c in m, and L_ℓ/L_e, in m/m

In this correlation the low value of the exponent of $\dot{q}''_{cwi}$ of 0.0861 indicates that the wall heat flux does not play an important role in determining the condenser heat transfer coefficient. The liquid charge fill ratio however is significant with a relatively large magnitude of 0.3474 for the exponent of L_ℓ/L_e.

A similar correlation for the inclined case (122 data points $r^2 = 46.9\%$) was obtained as:

$$h_{cwi} = 29.78\,(\dot{q}''_{cwi}) - 0.03941\,(P_i)^{-0.2717}\,(L_c)^{-0.6661} \times (L_\ell/L_e)^{-0.01131}\,(\sin\phi)^{-0.3821} \quad (9)$$

In this correlation it is again seen that the heat flux is not important in determining the condensation heat transfer coefficient. P_i and L_c and ϕ are however significant. The effect of the amount of liquid in the thermosyphon as reflected by L_ℓ/L_e although significant in the case of a vertical thermosyphon is however not at all significant in the inclined orientation. This may not be surprising because i) the propensity for condensate to be expelled from the evaporator of a vertical thermosyphon is significantly greater than for an inclined thermosyphon; ii) the occurrence of spasmodic flooding and geysering episodes does not limit the maximum heat transfer rate of a thermosyphon as the temperature difference between the hot and cold ends increases and at least initially the heat transfer rate increases yet further before reaching a maximum; and iii) the more liquid in the condenser the thicker the average film thickness of liquid between the vapour and the wall and hence the greater the thermal resistance of the liquid.

The variation of the predicted condenser heat transfer using equations (8) and (9) from the experimentally determined values is shown in Figure 7 to be within $\pm 15\%$.

The square of the correlation coefficient as given by $r^2 = 46.9\%$ for equation (9) is relatively low Different correlating equations were attempted to correlate the data. A better correlation (122 data points, $r^2 = 66.4\%$) was obtained by including the theoretical value for an inclined thermosyphon as given by equation (8) and adjusting it with the angle and condenser length as

$$h_{cwi} = 8.585 \left(h_{cwi,eq(8)}\right)^{0.3566} (L_c)^{-0.6946} (\sin\phi)^{-0.1568} \tag{10}$$

The predicted values as given by equations (9) and (10) are compared with each other in Figure 8.

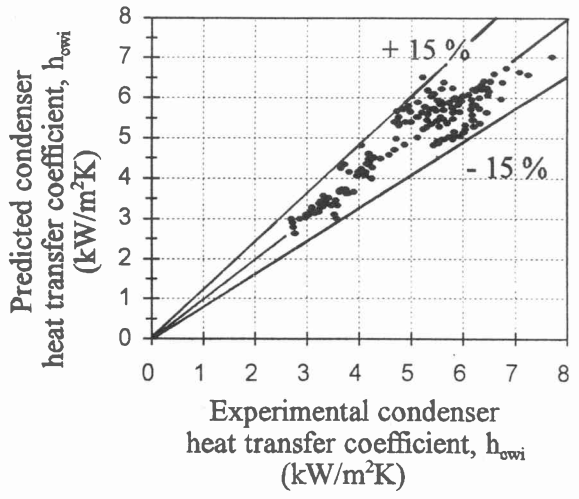

Figure 7 Predicted condenser heat transfer coefficient using equations (8) and (9) compared with the experimentally determined values

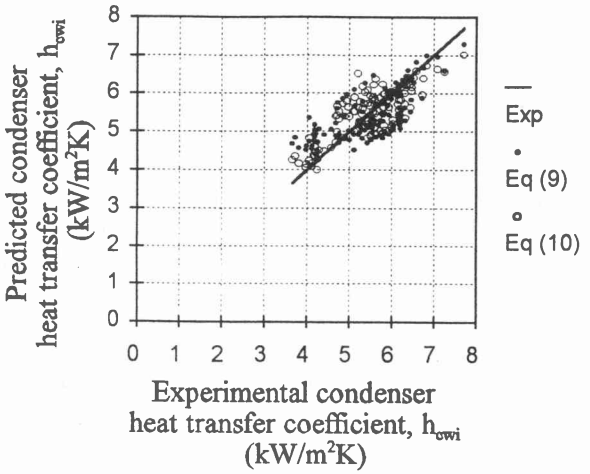

Figure 8 Comparison of the two predicted condenser transfer coefficients for the inclined orientation using equations (9) and (10) compared with the experimentally determined values

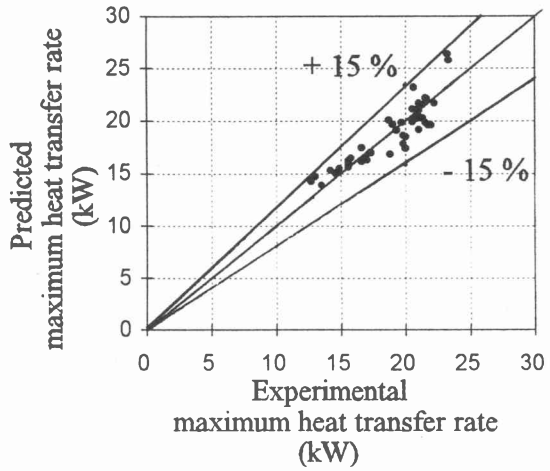

Figure 9 Predicted maximum heat transfer rate using equation (12) compared with the experimentally determined values

$$V_{sv,\max} = 136.2 (T_i)^{-0.718} (\phi)^{-0.429} (L_\ell/L_e)^{-0.108} \tag{11}$$

where $V_{sv,\max}$ is in m/s if T_i is in °C and ϕ in °. $V_{sv,\max}$ increases significantly as ϕ decreases, for instance at $T_i = 30°C$, $V_{sv,\max} = 1.6$ m/s for the vertically orientated thermosyphon, whereas for $\phi = 30°$ $V_{sv,\max}$ is some 72% greater at 2.75 m/s. The maximum heat transfer rate is then readily calculated using

$$\dot{q}_{\max} = \left(\pi d_i^2/4\right) \rho_v h_{fg} V_{sv,\max} \tag{12}$$

The variation of the predicted heat transfer rate using equation (12) from the experimentally determined values is shown in Figure 9 to be within 15%.

Discussion

Evaporator heat transfer coefficient

The evaporator heat transfer coefficients as given by the equations (6) and (7) are plotted in Figure 10 for more or less average values of the internal pressure, liquid charge fill ratio and liquid length of $P_i = 11.67$ bar (30°C), $L_\ell/L_e = 0.458$ and $L_\ell = 400$ mm . The evaporator heat transfer coefficient is plotted as a function of the evaporator heat flux up to the maximum evaporator heat flux. It is seen that although the maximum heat transfer rate increases as the angle of inclination to the horizontal decreases with a peak at about 60° that the heat transfer coefficient actually decreases.

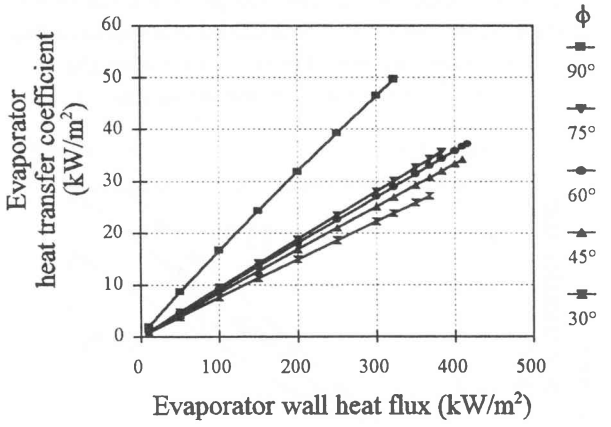

Figure 10 Predicted evaporator heat transfer coefficient as a function of the evaporator wall heat flux for different inclination angles ϕ for $P_i = 11.67$ bar (30°C), $L_\ell = 400$ mm and $L_\ell/L_e = 0.458$

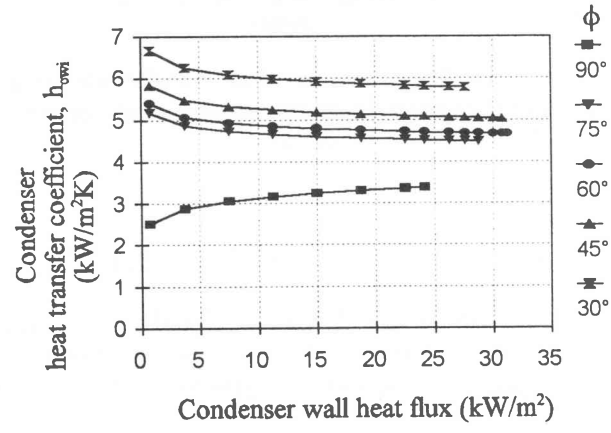

Figure 11 Predicted condenser heat transfer coefficient as a function of the condenser wall heat flux for different inclination angles ϕ for $P_i = 11.67$ bar (30°C), $L_\ell = 400$ mm and $L_\ell/L_e = 0.458$

The experimentally determined evaporator heat transfer coefficients for $\phi = 90°$ were compared to a number of available correlations. A correlation for boiling of ammonia in a vertical pool is available.[8,9] The experimentally determined values for $L_\ell/L_e = 1$ and $L_\ell = 400$ mm were 52±3% higher. This is expected because existing equations for pool boiling assume a relatively large pool in which the heated surface is placed. In a thermosyphon however the boiling takes place in a relatively long and narrow pipe which in this case is $L_\ell/d_i = 400/32 = 12.5$.

Other correlations have been proposed for the evaporator heat transfer coefficient for vertically orientated thermosyphons.[3,10,11] The data sets used to determine these correlations do not appear to contain arrimonia as working fluid. It may be for this reason that heat transfer coefficients using El-Genk and Saber's correlations yielded values of 230±40 % higher than the present experimental values. Values using correlations by Imura and Negishi and Shiraishi were all on average some 57% lower that the present experimental values.

Condenser heat transfer coefficient

The condenser heat transfer coefficients as given by the equations (8) and (9) are plotted in Figure 11 also for more or less average values of the internal pressure, liquid charge fill ratio and liquid length of $P_i = 11.67$ bar (30°C), $L_\ell/L_e = 0.458$ and $L_\ell = 400$ mm . The condenser heat transfer coefficient is plotted as a function of the condenser heat flux up to the maximum heat transfer rate. It is seen that, in contrast to the evaporator, the condenser heat transfer coefficient increases as the angle of inclination to the horizontal decreases.

Assuming that the condensate flows as a laminar film on the inside wall of the condenser the condensation heat transfer coefficient can be theoretically determined. The condensation heat transfer coefficient may be defined as the wall heat flux divided by the average temperature difference as

$$h_{wci} = \frac{\dot{q}''}{(1/A_{wci}) \int T_{wci} dA - T_i} \tag{13}$$

where $\dot{q}''$ is the heat flux and $(1/A_{wci}) \int T_{wci} dA$ is the average inside wall temperature of the condenser. Using this definition of the average heat transfer coefficient an equation for a vertical orientation can be derived as

$$h_{wci} = 2.64 \left(\frac{k_\ell^3 \rho_\ell^2 h_{fg}}{\mu_\ell} \cdot \frac{1}{L_c \dot{q}''} \right)^{1/3} \tag{14}$$

This equation shows that the thermal conductivity of the liquid phase of the working fluid, k_ℓ plays the dominant role in the condensation heat transfer coefficient. This is followed by the density of the liquid. The latent heat of vaporisation, liquid viscosity, condenser length and the condenser wall heat flux each have an equal but lesser influence on the condensation heat transfer coefficient.

For a relatively long inclined pipe (neglecting the effect of the extra condensate that drains from the wall and runs as a rivulet in the bottom of the tube) the condensa-

tion heat transfer coefficient is derived as:

$$h_{wci} = 1.30 \left(\frac{k_\ell^3 \rho_\ell^2 h_{fg}}{\mu_\ell} \cdot \frac{\cos\phi}{d_i \dot{q}''} \right)^{1/3} \quad (15)$$

The equation for the vertical case gives reasonable results but the equation for the inclined case tends to give values that are too high as shown in Figure 12.

A number of experimentally determined correlations are available in the literature. The correlations are limited in the sense that they are invariably for vertical orientations and none include ammonia as working fluid in their data sets. Three such correlations attributable to Hirashima *et al.*,[12] Uehara,[13] and Gross[13] are compared to the experimentally determined results shown in Figure 13.

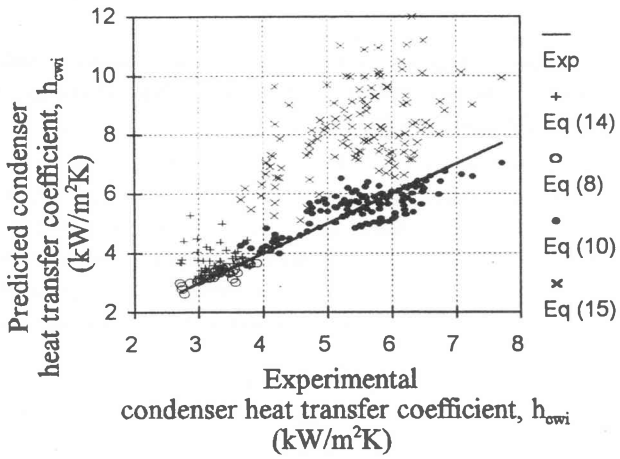

Figure 12 Predicted condenser heat transfer coefficient using film theory and the correlated predictions compared with the experimentally determined values

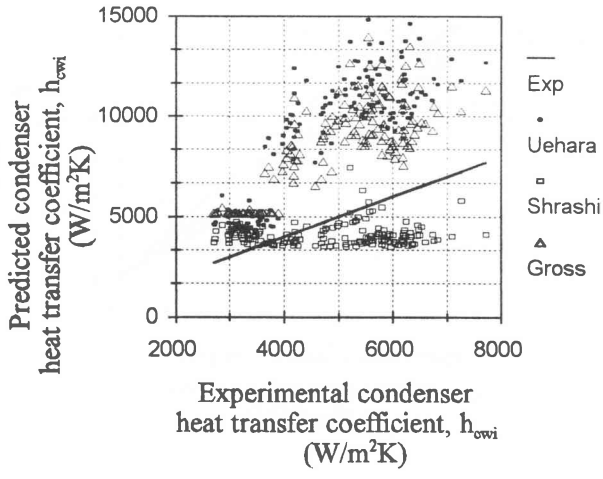

Figure 13 Predicted condenser heat transfer coefficient using various existing correlations compared with the experimentally determined values

Hirashima's correlation (which was originally determined using water as the working fluid) gives a constant value of 4 kW/m^{2}K when applied to ammonia and operating conditions similar to those upon which the experimental results were obtained. The Uehara and Gross correlations give heat transfer coefficients that are consistently higher than the experimental values.

Overall heat transfer resistance

The maximum heat transfer rate increases as the thermosyphon is tilted from a vertical orientation On the other hand the actual heat transferred is relatively insensitive to the inclination angle. This is because the evaporator heat transfer coefficient decreases whilst the condensation heat transfer coefficient increases, as shown in Figures 10 and 11.

Conclusions

The experimentally obtained evaporator and condenser heat transfer coefficients and the maximum heat transfer rate were suitably correlated by equations (6) to (12). The predicted values using these correlations corresponded reasonably well to the experimentally determined values as shown in Figures 6, 7, and 8. The evaporator heat transfer coefficient scatter was 30%, the condenser heat transfer coefficient scatter was ±15% and for the maximum heat transfer rate it was also within 15%.

The experimentally determined heat transfer coefficients did not correspond well with existing correlations gleaned from the available published literature. This is attributed to the limited availability of data pertaining to ammonia and inclined orientations in the data-sets upon which the existing correlations are based. Another reason for this could be due to the complex and uncertain nature of the heat transfer mechanisms taking place in a thermosyphon. The thermosyphon tested is relatively long and it is possible that a number of mechanisms, as shown in Figure 1, may be taking place simultaneously in different portions of the evaporator. Yet another reason could be that the occurrence of flooding (especially in inclined orientations of a thermosyphon) does not necessarily constitute a state of maximum heat transfer. The heat transfer coefficients for operation under flooded conditions cannot be expected to be the same as under conditions where the liquid is flowing under relatively laminar flowing films, either as films on the walls of the tube or as a rivulet along the bottom of the tube.

References

1. Faghri A. *Heat Pipe Science and Technology.* Taylor& Francis, 1995.
2. Dobson RT & Kröger DG. Effect of evaporator surface on the maximum heat transfer rate of an inclined two-phase closed thermosyphon. *10th Int. Heat Pipe Conf.*, Stuttgart, September 22–25, 1997.

3. Pioro LS & Pioro IL. *Industrial Two-phase Thermosyphons.* Begell house, New York, 1997.

4. Aburghaia MA. Analysis and application on correlations of critical heat flux in a closed two-phase thermosyphon. *5th Int. Heat Pipe Symposium*, Melbourne, 17–20 November 1996.

5. Ohadi MM, Li SS, Radermacher R & Dessiatoun S. Critical review of available correlations for two-phase flow heat transfer of ammonia. *Int. J Refrig.*, **19**, pp.272–284, 1996.

6. Dobson RT & Kröger DG. Determination of the heat transfer coefficient for a tube in tube heat exchanger. Submitted to *Int J Mech Eng Education*, 1999.

7. Dobson RT & Kröger DG. Evaporator heat transfer coefficient and maximum heat transfer rate of an ammonia-charged inclined two-phase closed-thermosyphon. *11th Int. Heat Pipe Conf.*, Tokyo, 12–16 September 1999.

8. Stephan K. *Heat Transfer in Condensation and Boiling.* Springer-Verlag, 1992.

9. Stephan K & Abdelsalam M. Heat transfer correlations for natural convection boiling. *Int J Heat Mass Transfer*, **23**, pp.73–87, 1980.

10. El-Genk MS & Saber HH. Heat transfer correlations for liquid film in the evaporator of enclosed, gravity-assisted thermosyphons. *J Heat Transfer*, **120**, pp.477-484, 1998.

11. Negishi K *et al.* Heat-transfer of a corrugated-tube thermosiphon [sic], Part I Evaporator performance. *Heat Transfer-Japanese Research*, **20**, pp.144–157, 1991.

12. Hirashima M *et al.* Heat-transfer performance of corrugated-tube thermosiphons [sic], Part 2 Condenser performance. *Heat Transfer-Japanese Research*, **20**, pp.158–168, 1991.

13. Gross U. Reflux condensation heat transfer inside a closed thermosyphon. *Int J Heat Mass Transfer*, **35**, pp.279–294, 1992.